INTERNATIONAL JOURNAL FOR NUMERICAL METHODS IN FLUIDS
Int. J. Numer. Meth. Fluids 2005; **49**:817–835
Published online 3 August 2005 in Wiley InterScience (www.interscience.wiley.com). DOI: 10.1002/fld.1020

Explicit algebraic stress modelling of homogeneous and inhomogeneous flows

T. H. Chiu[1], L. K. Yeh[1], C. A. Lin[1,*,†] and S. J. Chern[2]

[1]*Department of Power Mechanical Engineering, National Tsing Hiua University, Hsinchu 300, Taiwan*
[2]*Department of Mathematics, National Tsing Hiua University, Hsinchu 300, Taiwan*

SUMMARY

Capability of the explicit algebraic stress models to predict homogeneous and inhomogeneous shear flows are examined. The importance of the explicit solution of the production to dissipation ratio is first highlighted by examining the algebraic stress models performance at purely irrotational strain conditions. Turbulent recirculating flows within sudden expanding pipes are further simulated with explicit algebraic stress model and anisotropic eddy viscosity model. Both models predict better stress–strain interactions, showing reasonable shear layer developments. The anisotropic stress field are also accurately predicted by the models, though the anisotropic eddy viscosity model of Craft *et al*. returns marginally better results. Copyright © 2005 John Wiley & Sons, Ltd.

KEY WORDS: turbulent flows; turbulence modelling; explicit algebraic stress model; homogeneous shear flow; sudden expanding pipe flow

1. INTRODUCTION

It is widely accepted that the linear eddy–viscosity type of turbulence models cannot, without modifications, account for the streamline curvature effect. Therefore, the natural route is to apply second-moment closures in predicting the recirculating flows [1, 2]. However, the extra computational cost incurred due to the solution of the transport equations of the Reynolds stresses prevents the model from being widely used, especially in three-dimensional environments.

One alternative is to adopt a non-linear stress and strain relationship of the Reynolds stresses. This can be achieved by assuming that the Reynolds stresses are taken to be non-linear function of the mean velocity gradients. However, there are many approaches in deriving the coefficients and determining the order of the tensorially independent groups. Most of the

*Correspondence to: C. A. Lin, Department of Power Mechanical Engineering, National Tsing Hiua University, Hsinchu 300, Taiwan.
†E-mail: calin@pme.nthu.edu.tw

Contract/grant sponsor: National Science Council; contract/grant number: NSC-89-2212-E-007-030

Received 22 January 2004
Revised 4 November 2004
Accepted 17 May 2005

models are formulated at the quadratic level [3], and few adopt cubic stress and strain relationships [4, 5]. These models are termed by Gatski and Speziale [6] as the anisotropic eddy viscosity models, because these formulations have no direct relation with the Reynolds stress models. Kuo *et al.* [7] investigated the capability of different quadratic [3] and cubic [4, 5] anisotropic eddy viscosity models to predict recirculating flows and the cubic model of Craft *et al*. was shown to perform best.

Based on the algebraic stress model (ASM) of Rodi [8] and with the aid of the Caley–Hamilton theorem, Pope [9] proposed that the most general form of anisotropy tensor can be expressed in terms of the mean strain and vorticity tensors of 10 tensorially independent groups (up to fifth order) and coefficients. This was motivated by the fact that the implementations of the algebraic stress models are not straightforward, because the stress–strain relation is not explicit. The explicit algebraic stress models are attractive, because the Reynolds stresses are related to the mean velocity gradients implicitly through the Reynolds stress closures.

Gatski and Speziale [6] further extended Pope's formulation to three-dimensional turbulent flows in non-inertial frame. One drawback of the above model is the adoption of the equilibrium value of the ratio of production to dissipation ($P/\varepsilon = 1.89$) in the model coefficients. This, as pointed out by Girimaji [10], is internally inconsistent. In order to account for the turbulent flows with localized strain rates that are large, the Gatski and Speziale's explicit algebraic stress model has been regularized. Girimaji has indicated that the production to dissipation ratio can in fact be determined analytically, and this has potential benefits in computing complex flows with strong shear layers.

Therefore, the focus of the study is to examine the importance of the explicit solution of the P/ε ratio at large strain rates for explicit algebraic stress models. Also, the cubic anisotropic model of Craft *et al*. is also adopted here to examine its performance relative to the explicit algebraic stress models. Attention will be first focusing on the models' performance in homogeneous flow under rotational and irrotational strains. The capability of the explicit algebraic stress model and anisotropic eddy viscosity model to predict inhomogeneous flow within the sudden expanding pipe geometry is also investigated.

2. THE COMPUTATIONAL MODEL

2.1. The governing equations

The behaviour of the flow is in general governed by the fundamental principles of classical mechanics expressing the conservation of mass and momentum. The time-averaged equations for high-Reynolds-number flow, may be described by the equations (in Cartesian tensor):

$$\frac{\partial(U_i)}{\partial x_i} = 0 \tag{1}$$

$$\frac{\partial(U_i U_j)}{\partial x_j} = -\frac{1}{\rho}\frac{\partial P}{\partial x_i} + \frac{\partial}{\partial x_j}\left[\nu\left(\frac{\partial U_i}{\partial x_j} + \frac{\partial U_j}{\partial x_i}\right) - \overline{u_i u_j}\right] \tag{2}$$

where $\overline{u_i u_j}$ is Reynolds stress arising from the time-averaging process. The modelling of the Reynolds stress is addressed in the next section.

2.2. Turbulence models

In the present application, the non-linear eddy viscosity model is employed to model the Reynolds stress. The first model variant adopted is the anisotropic eddy viscosity model of Craft *et al.* [4], where the Reynolds stresses are expressed as the non-linear combination of the strain rates.

$$\begin{aligned} b_{ij} &= \left[\frac{\overline{u_i u_j}}{2k} - \frac{1}{3}\delta_{ij}\right] \\ &= -C_\mu S_{ij} + C_1 C_\mu \left[S_{ik}S_{kj} - \frac{1}{3}\delta_{ij}S_{kl}S_{kl}\right] + C_2 C_\mu [W_{ik}S_{kj} + W_{jk}S_{ki}] \\ &\quad + C_3 C_\mu \left[W_{ik}W_{kj} - \frac{1}{3}\delta_{ij}W_{kl}W_{kl}\right] + C_4 C_\mu^2 \left(S_{ki}W_{lj} + S_{kj}W_{li} - \frac{2}{3}S_{km}W_{lm}\delta_{ij}\right)S_{kl} \\ &\quad + C_6 C_\mu^2 S_{ij}S_{kl}S_{kl} + C_7 C_\mu^2 S_{ij}W_{kl}W_{kl} \end{aligned} \tag{3}$$

where $C_1 = -0.2,\ C_2 = 0.2,\ C_3 = 0.52,\ C_4 = -4,\ C_6 = -0.4,\ C_7 = 0.4.$

$$C_\mu = \frac{0.3}{1. + 0.35[\max(S,\Omega)]^{1.5}}[1 - \mathrm{e}^{[-0.36/\mathrm{e}^{-0.75\ \max(S,\Omega)}]}]$$

$$S_{ij} = \frac{1}{2}\frac{k}{\varepsilon}\left(\frac{\partial U_i}{\partial x_j} + \frac{\partial U_j}{\partial x_i}\right), \quad W_{ij} = \frac{1}{2}\frac{k}{\varepsilon}\left(\frac{\partial U_i}{\partial x_j} - \frac{\partial U_j}{\partial x_i}\right)$$

$$S = \sqrt{2S_{ij}S_{ij}}, \quad \Omega = \sqrt{2W_{ij}W_{ij}}$$

Another adopted approach is the explicit solution of the algebraic stress model (ASM) of Rodi [8]. The Reynolds stress transport equation can be expressed as

$$\underbrace{\frac{\partial}{\partial x_k}(U_k\overline{u_i u_j})}_{C_{ij}} - \underbrace{\frac{\partial}{\partial x_k}\left[\nu\frac{\partial \overline{u_i u_j}}{\partial x_k} - \overline{u_i u_j u_k} - \frac{1}{\rho}(\overline{pu_i}\delta_{jk} + \overline{pu_j}\delta_{ik})\right]}_{d_{ij}}$$

$$= \underbrace{-\overline{u_i u_k}\frac{\partial U_j}{\partial x_k} - \overline{u_j u_k}\frac{\partial U_i}{\partial x_k}}_{P_{ij}} + \underbrace{\overline{\frac{p}{\rho}\left(\frac{\partial u_i}{\partial x_j} + \frac{\partial u_j}{\partial x_i}\right)}}_{\phi_{ij}} - \underbrace{\left(\frac{2}{3}\delta_{ij}\varepsilon + \varepsilon_{ij,D}\right)}_{\varepsilon_{ij}} \tag{4}$$

where C_{ij}, d_{ij}, P_{ij} and ε_{ij} represent the convection, diffusion generation and dissipation of Reynolds stress and ϕ_{ij} stands for the pressure-strain correlation. Here the ε_{ij} has been split into isotropic and devatoric part.

The contraction of the above equation results in the transport equation of turbulence kinetic energy $k = \overline{u_i u_i}/2$.

$$\underbrace{\frac{\partial}{\partial x_j}(U_j k)}_{C_k} - \underbrace{\frac{\partial}{\partial x_j}\left(\nu\frac{\partial k}{\partial x_j} - \frac{1}{2}\overline{u_i u_i u_j} - \frac{1}{\rho}\overline{p u_j}\right)}_{d_k} = \underbrace{-\overline{u_i u_j}\frac{\partial U_i}{\partial x_j}}_{P} - \varepsilon \tag{5}$$

The algebraic simplification of the Reynolds stress transport equation is expressed as

$$C_{ij} - d_{ij} = \frac{\overline{u_i u_j}}{k}(C_k - d_k) = \frac{\overline{u_i u_j}}{k}(P - \varepsilon) \tag{6}$$

Thus, Equation (4) can be rewritten as

$$\frac{\overline{u_i u_j}}{k}(P - \varepsilon) = P_{ij} - \frac{2}{3}\delta_{ij}\varepsilon + \underbrace{\phi_{ij} - \varepsilon_{ij,D}}_{\pi_{ij}} \tag{7}$$

The most general form of π_{ij} in the linear anisotropy tensor b_{ij} [11] can be expressed as

$$\begin{aligned}\pi_{ij} = &-\left(C_1^0 + C_1^1\frac{P}{\varepsilon}\right)\varepsilon b_{ij} + C_2\varepsilon S_{ij} + C_3\varepsilon\left(b_{ik}S_{jk} + b_{jk}S_{ik} - \frac{2}{3}b_{mn}S_{mn}\delta_{ij}\right)\\ &+C_4\varepsilon(b_{ik}W_{jk} + b_{jk}W_{ik})\end{aligned} \tag{8}$$

Thus, the final form of the algebraic stress model can be expressed as

$$\begin{aligned}b_{ij}\left[(C_1^0 - 2) + (C_1^1 + 2)\frac{P}{\varepsilon}\right] = &\left(C_2 - \frac{4}{3}\right)S_{ij} + (C_3 - 2)\left(b_{ik}S_{jk} + b_{jk}S_{ik} - \frac{2}{3}b_{mn}S_{mn}\delta_{ij}\right)\\ &+(C_4 - 2)(b_{ik}W_{jk} + b_{jk}W_{ik})\end{aligned} \tag{9}$$

Following Gatski and Speziale [6], the two-dimensional explicit algebraic stress model can be written as

$$b_{ij} = -\frac{3}{3 - 2\eta_1 - 6\eta_2}\left[\beta_1 S_{ij} + \beta_2(S_{ik}W_{kj} + S_{jk}W_{ki}) - 2\beta_3\left(S_{ik}S_{kj} - \frac{1}{3}S_{kl}S_{kl}\delta_{ij}\right)\right] \tag{10}$$

where $\beta_1 = (4/3 - C_2)/\beta_4$, $\beta_2 = \beta_1(2 - C_4)/\beta_4$, $\beta_3 = \beta_1(2 - C_3)/\beta_4$, $\beta_4 = (C_1^0 - 2) + (C_1^1 + 2)P/\varepsilon$, $\eta_1 = \xi_1(2 - C_3)^2/\beta_4^2$ and $\eta_2 = \xi_2(2 - C_4)^2/\beta_4^2$. $\xi_1 = S_{ij}S_{ij}$ and $\xi_2 = W_{ij}W_{ij}$.

In the present study, the linear pressure-strain model adopted is the SSG model [12]. The model coefficients are $C_1^0 = 3.4$, $C_1^1 = 1.8$, $C_2 = 0.36$, $C_3 = 1.25$ and $C_4 = 0.4$.

It was indicated by Gatski and Speziale [6] that for sufficiently large strain rates η_1, singularities can occur. Therefore, the regularized model is proposed by Gatski and Speziale, i.e.

$$b_{ij} = \frac{3(1 + \eta_1)}{3 + \eta_1 + 6\eta_2(1 + \eta_1)}\left[\beta_1 S_{ij} + \beta_2(S_{ik}W_{kj} + S_{jk}W_{ki}) - 2\beta_3\left(S_{ik}S_{kj} - \frac{1}{3}S_{kl}S_{kl}\delta_{ij}\right)\right] \tag{11}$$

This new formulation ensures the coefficient to be positive. However, there remains unknown ratio of P/ε. To propose an explicit ASM, the equilibrium value of $P/\varepsilon = 1.89$ is adopted by Gatski and Speziale [6]. This, as pointed out by Girimaji [10], is internally inconsistent, because $-\overline{u_i u_j}(\partial U_i/\partial x_j)/\varepsilon \neq 1.89$ away from equilibrium condition.

An alternative approach was proposed by Girimaji [10], where the ratio of P/ε for two dimensional flow is obtained analytically. If Equation (10) is rewritten as

$$b_{ij} = \beta_1^* S_{ij} + \beta_2^*(S_{ik}W_{kj} + S_{jk}W_{ki}) + \beta_3^*(S_{ik}S_{kj} - \tfrac{1}{3}S_{kl}S_{kl}\delta_{ij}) \tag{12}$$

where $\beta_1^* = g\beta_1$, $\beta_2^* = g\beta_2$, $\beta_3^* = -2g\beta_3$ and $g = -3/(3 - 2\eta_1 - 6\eta_2)$.

By multiplying the S_{ij} to the above equation, it can be shown that,

$$\frac{P}{\varepsilon} = -2b_{ij}S_{ij} = -2\beta_1^*\xi_1 \tag{13}$$

Therefore, P/ε is a function of β_1^* and strain rates ξ_1. By replacing b_{ij} and P/ε with Equations (12) and (13), Equation (9) can be written as

$$\begin{aligned}
&[C_1^0 - 2 - 2(C_1^1 + 2)\xi_1\beta_1^*]\left[\beta_1^* S_{ij} + \beta_2^*(S_{ik}W_{kj} + S_{jk}W_{ki}) + \beta_3^*\left(S_{ik}S_{kj} - \frac{1}{3}S_{kl}S_{kl}\delta_{ij}\right)\right] \\
&\quad = \left[C_2 - 4/3 + \frac{\xi_1}{3}(C_3 - 2)\beta_3^* + 2\xi_2(C_4 - 2)\beta_2^*\right]S_{ij} \\
&\qquad + 2(C_3 - 2)\beta_1^*\left(S_{ik}S_{kj} - \frac{1}{3}S_{kl}S_{kl}\delta_{ij}\right) - (C_4 - 2)\beta_1^*(S_{ik}W_{kj} + S_{jk}W_{ki})
\end{aligned} \tag{14}$$

By comparing the coefficients of the three strain rates, S_{ij}, $S_{ik}W_{kj} + S_{jk}W_{ki}$ and $S_{ik}S_{kj} - \frac{1}{3}S_{kl}S_{kl}\delta_{ij}$, three equations can be obtained, i.e.

$$\beta_1^*[C_1^0 - 2 - 2(C_1^1 + 2)\xi_1\beta_1^*] = C_2 - 4/3 + \frac{\xi_1}{3}(LC)\beta_3^* + 2\xi_2(C_4 - 2)\beta_2^* \tag{15}$$

$$\beta_2^* = \frac{-(C_4 - 2)\beta_1^*}{C_1^0 - 2 - 2(C_1^1 + 2)\xi_1\beta_1^*}, \quad \beta_3^* = \frac{2(C_3 - 2)\beta_1^*}{C_1^0 - 2 - 2(C_1^1 + 2)\xi_1\beta_1^*} \tag{16}$$

The above equations can be used to solve the three unknowns. By replacing β_2^* and β_3^* in Equation (15) using Equation (16), a cubic equation for β_1^* can be obtained and is as follows:

$$\begin{aligned}
&[2(C_1^1 + 2)\xi_1]^2\beta_1^{*3} - [4\xi_1(C_1^0 - 2)(C_1^1 + 2)]\beta_1^{*2} \\
&\quad + [(C_1^0 - 2)^2 + 2(C_1^1 + 2)(C_2 - 4/3) - \tfrac{2}{3}\xi_1(C_3 - 2)^2 + 2\xi_2(C_4 - 2)^2] \\
&\quad \times \beta_1^* - (C_1^0 - 2)(C_2 - 4/3) = 0
\end{aligned} \tag{17}$$

The general feasible solutions of this equation were obtained by Girimaji [10] and are listed below.

$$\beta_1^* = \begin{cases} \dfrac{(C_1^0-2)(C_2-4/3)}{(C_1^0-2)^2+2\xi_2(C_4-2)^2} & \text{for } \xi_1 = 0 \\ \dfrac{(C_1^0-2)(C_2-4/3)}{(C_1^0-2)^2-2/3\xi_1(C_3-2)^2+2\xi_2(C_4-2)^2} & \text{for } C_1^1+2=0 \\ -\dfrac{p}{3}+\left(-\dfrac{b}{2}+\sqrt{D}\right)^{1/3}+\left(-\dfrac{b}{2}-\sqrt{D}\right)^{1/3} & \text{for } D>0 \\ -\dfrac{p}{3}+2\sqrt{-\dfrac{a}{3}}\cos\left(\dfrac{\theta}{3}\right) & \text{for } D<0 \text{ and } b<0 \\ -\dfrac{p}{3}+2\sqrt{-\dfrac{a}{3}}\cos\left(\dfrac{\theta}{3}+\dfrac{2\pi}{3}\right) & \text{for } D<0 \text{ and } b>0 \end{cases} \tag{18}$$

where

$$p = -\frac{2(C_1^0-2)}{\xi_1(C_1^1+2)}$$

$$q = \frac{(C_1^0-2)^2+\xi_1(C_1^1+2)(C_2-4/3)-2/3\xi_1(C_3-2)^2+2\xi_2(C_4-2)^2}{[\xi_1(C_1^1+2)]^2}$$

$$r = -\frac{(C_1^0-2)(C_2-4/3)}{[\xi_1(C_1^1+2)]^2}$$

$$a = q-\frac{p^2}{3}$$

$$b = (2P^3-9pq+27r)/27$$

$$D = \frac{b^2}{4}+\frac{a^3}{27}$$

$$\cos(\theta) = -\frac{b}{2\sqrt{-a^3/27}}$$

It should be pointed out that by adopting this approach, no regularization procedure is needed, because the approach produces non-singular behaviour [10, 13].

The k and ε in the above explicit algebraic stress closure are obtained by solving the modelled transport equations. The equations can be expressed as

$$\frac{\partial U_j k}{\partial x_j} = \frac{\partial}{\partial x_j}\left[\nu_t \frac{\partial k}{\partial x_j}\right] - \overline{u_i u_j}\frac{\partial U_i}{\partial x_j} - \varepsilon \tag{19}$$

$$\frac{\partial U_j \varepsilon}{\partial x_j} = \frac{\partial}{\partial x_j}\left[\frac{\nu_t}{\sigma_\varepsilon}\frac{\partial \varepsilon}{\partial x_j}\right] - C_{\varepsilon 1}\frac{\varepsilon}{k}\overline{u_i u_j}\frac{\partial U_i}{\partial x_j} - C_{\varepsilon 2}\frac{\varepsilon^2}{k} \tag{20}$$

where $C_{\varepsilon 1}$, $C_{\varepsilon 2}$ and σ_ε are 1.44, 1.92 and 1.3, respectively. When adopting the SSG model, the value of $C_{\varepsilon 2}$ in the ε equation is modified to be 1.83 [12].

3. NUMERICAL ALGORITHM

This scheme solves discretized versions of all equations on a staggered finite-volume arrangement. The principle of mass-flux continuity is imposed indirectly via the solution of pressure-correction equations according to the SIMPLE algorithm [14]. The flow-property values at the volume faces contained in the convective fluxes which arise from the finite-volume integration process are approximated by the QUICK scheme [15].

At the wall, the wall-parallel velocity components U was assumed to vary logarithmically between the semi-viscous sublayer, at $y_v^+ = 11.2$, and the first computational node lying in the region $30 < y^+ < 100$. This treatment yielded boundary conditions for the shear stresses and also permitted the volume-averaged near-wall generation rates of the tangential normal stresses to be computed over the associated near-wall finite volumes (the generation of the wall-normal intensity was assumed negligibly small). The linear variation of the turbulent length scale, $L = \kappa y / C_\mu^{3/4}$, in the log-law region, together with $\varepsilon = k^{3/2}/L$, and the invariant value $\varepsilon = 2\mu_l k_v/(\rho y_v^2)$ in the viscous sublayer, allowed the volume-averaged dissipation rate to be determined; details may be found in Reference [16]. This same L-variation was also used to prescribe explicitly the dissipation rate at the near-wall computational node, serving as the boundary condition for inner-field cells.

The numerical meshes, 178×118 and 90×60, are non-uniform both in the x and y directions, where clustered meshes are present in the recirculation zone and shear layers. Initial tests on the influences of the grid density revealed that the differences between the two meshes were small. Therefore, in subsequent computations, the mesh 90×60 will be adopted.

4. RESULTS

4.1. Homogeneous shear flows

The performance of the model is first examined by applying to the homogeneous shear flow in equilibrium state at different strain rates

$$2S_{ij} = \begin{pmatrix} 0 & S & 0 \\ S & 0 & 0 \\ 0 & 0 & 0 \end{pmatrix}$$

The anisotropy a_{ij} is defined as $\overline{u_i u_j}/k - 2/3\delta_{ij}$. The predicted results are contrasted with DNS data [17] and measurements [18–20]. Three models are contrasted here, namely SSG, SSG–GS and Craft *et al*. The SSG–GS is the regularized explicit ASM model by Gatski and Speziale (shown in Equation (11)), while the SSG is the fully explicit ASM, i.e. the P/ε is obtained

by Equation (13). As shown in Figure 1, it can be clearly seen that all the models perform reasonably well, though at higher and lower strain rates the models behave differently.

Further, attention is directed to the homogeneous turbulence field induced by the irrotational strains under axi-symmetric contraction (A-C)

$$2S_{ij} = \begin{pmatrix} S & 0 & 0 \\ 0 & -S/2 & 0 \\ 0 & 0 & -S/2 \end{pmatrix}$$

and axi-symmetric expansion (A-E).

$$2S_{ij} = \begin{pmatrix} -S & 0 & 0 \\ 0 & S/2 & 0 \\ 0 & 0 & S/2 \end{pmatrix}$$

Here, the results by the fully explicit ASM and Craft *et al.*'s anisotropic eddy viscosity model are shown in Figures 2 and 3. The SSG–GS is not included because it produces unrealistic stress field. This is apparent by examining the regularized model, as shown in Equation (11). At high irrotational strain rates ($\eta_2 = 0$), the coefficient becomes constant, and the stress field is then proportional to $\beta_1 S_{ij}$, where β_1 is function of P/ε. For constant P/ε ratio, this implies

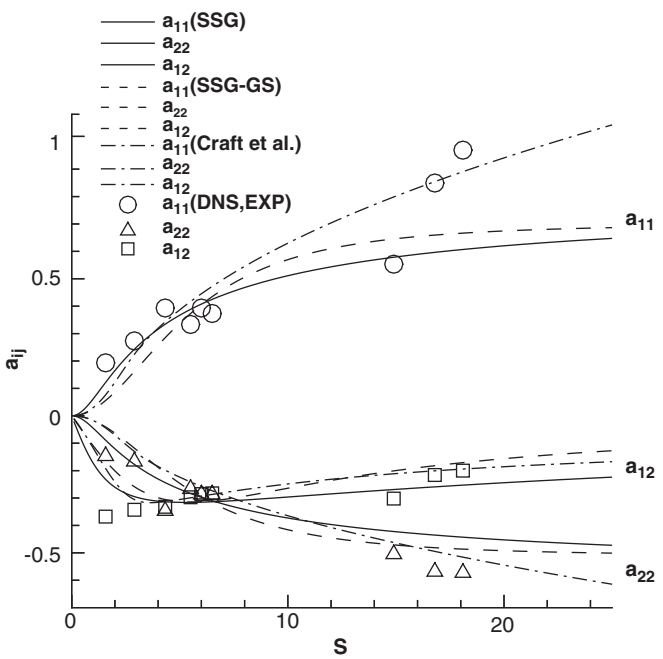

Figure 1. Variation of anisotropy at different strain rate—homogeneous shear.

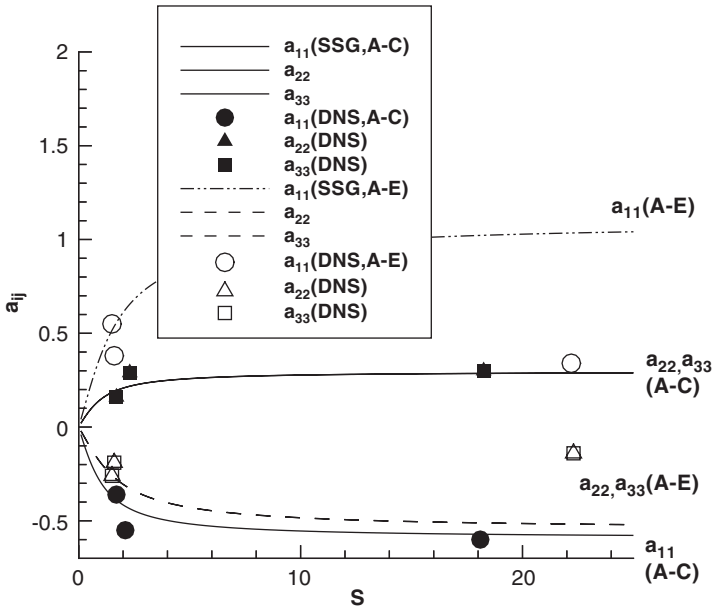

Figure 2. Anisotropy at different strain rate—axi-symmetric contraction and expansion (SSG model).

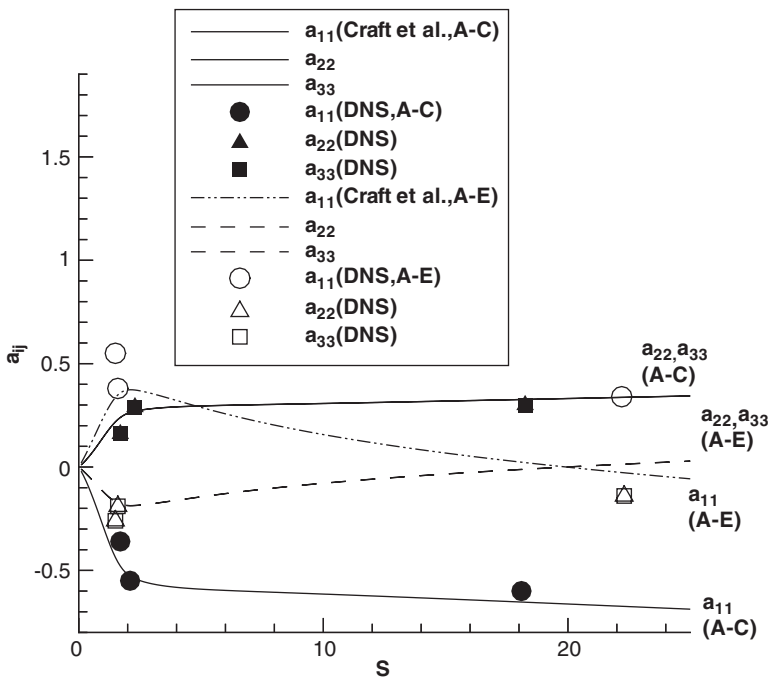

Figure 3. Anisotropy at different strain rate—axi-symmetric contraction and expansion (Craft *et al.*'s model).

that the $\beta_1 S_{ij}$ is again proportional to the strain rate (S_{ij}), and hence so is the case for the stress field. For the fully explicit ASM, the P/ε ratio increases in tandem with strain rates, and hence produces a bounded stress field. Another advantage of the explicit solution of the P/ε ratio is that the P/ε ratio is always positive and the coefficient for the S_{ij} in the stress and strain relation is always negative, which also ensures stable solution numerically.

For the axi-symmetric contraction case, the SSG model agrees well with the DNS data. However, for the axi-symmetric expansion case, the model produces a too high level of anisotropy at higher strain rates. These can be verified by examining the asymptotic anisotropy behaviours of the SSG model under the axi-symmetric contraction and expansion conditions. Chiu [21] found that the level of the asymptotic anisotropy is function of the model constants. The asymptotic formulations of the a_{ij} as derived by Chiu are listed below.

Asymptotic ($S=\infty$) anisotropy values under the axi-symmetric contraction:

$$a_{11} = \frac{2(-4+3C_2)}{3(2-C_3+\sqrt{12-6C_2-4C_3+C_3^2})} = -0.59 \tag{21}$$

$$a_{22} = a_{33} = \frac{4-3C_2}{3(2-C_3+\sqrt{12-6C_2-4C_3+C_3^2})} = 0.30 \tag{22}$$

Asymptotic ($S=\infty$) anisotropy values under the axi-symmetric expansion:

$$a_{11} = -\frac{2(-4+3C_2)}{3(-2+C_3+\sqrt{12-6C_2-4C_3+C_3^2})} = 1.09 \tag{23}$$

$$a_{22} = a_{33} = \frac{-4+3C_2}{3(-2+C_3+\sqrt{12-6C_2-4C_3+C_3^2})} = -0.55 \tag{24}$$

where the C_2 and C_3 are SSG model coefficients. As can be observed, the results agree perfectly with the numerical results at higher strain rates. It is also interesting to note that the values depend only on C_2 and C_3.

The Craft *et al.*'s model agrees perfectly with DNS data for the axi-symmetric contraction case, but produces the wrong trend under the axi-symmetric expansion condition. This can be verified by examining the model under the irrotational strains.

$$a_{ij} = \underbrace{-C_\mu S_{ij}}_{\text{(A)}} + \underbrace{C_1 C_\mu [S_{ik}S_{kj} - \tfrac{1}{3}\delta_{ij}S_{kl}S_{kl}]}_{\text{(B)}} + \underbrace{C_6 C_\mu^2 S_{ij}S_{kl}S_{kl}}_{\text{(C)}} \tag{25}$$

At the asymptotic state ($S=\infty$), C_μ is proportional to $S^{-3/2}$. Therefore, $a_{11} \sim -\sqrt{S}$ is always negative under either the axi-symmetric contraction or expansion strains, and is also not bounded. For the axi-symmetric expansion case, at low strain rates term (A) dominates, therefore a_{11} is positive. However at large strain rates term (B) is large, then a_{11} changes sign and becomes negative. It should be pointed out that a revised model proposed by

Craft *et al.* [22] including the transport equation for the second invariant, can deliver much better results.

4.2. Inhomogeneous shear flow—sudden expanding pipe flow

Next the computations are applied to a simple dump combustor with the expansion ratio of 1.5, as shown in Figure 4. The inlet centreline velocity was maintained at 19.2 m/s, corresponding to the Reynolds number of 1.25×10^5. The inlet of the computational domain was located at $X/H = 0.38$, which is the first downstream position at which measurements are available. H is the difference of the radius of the expanding and inlet pipe. The predicted results are contrasted with the measurements of Ahmed and Nejad [23]. Here, the high-Reynolds-number k–ε linear eddy–viscosity model of Jones and Launder [24] is also included for comparison purposes.

Figure 5 shows the predicted axial velocity distributions at four selected locations. It can be clearly seen that the linear k–ε model shows a more diffusive profile. The performance of the SSG and the anisotropic models shows the best results, where the shear layer is correctly predicted. The performance of the models can be further ascertained by reference to the shear stress distributions, shown in Figure 6. The correct development of the shear layer is the reflection of the accurate shear stress level predicted. The elevated level of diffusive cross stream transport of the k–ε prediction can be seen from the $\overline{uv}$ at $X/H = 2$. The performance of the anisotropic model is marginally better than the explicit algebraic stress model.

At $X/H = 2$, the SSG predicts a higher level of $\overline{uv}$ across the shear layer than that predicted by the Craft *et al.*'s model. This results in the faster development of the shear layer predicted by the SSG model, and hence lower levels of both mean velocity gradient and shear stress further downstream. Since the level of the turbulent kinetic energy is related to its generation term, where for simple shear flow is $P_k \sim -\overline{uv}\partial U/\partial y$, it is expected that at locations further downstream, the SSG predicted turbulence kinetic energy level should be lower than that predicted by the anisotropic model of Craft *et al.* This is verified by observing the predicted turbulence kinetic energy distributions as shown in Figure 7. The reduced level of SSG predicted shear stress at locations $X/H > 2$ is also clearly seen at Figure 6.

Figures 8–10 show the predicted turbulence intensity profiles. As expected, the linear model indicates an isotropic stress field. Both SSG ASM and the Craft *et al.*'s model show a better anisotropic stress field. The lower levels of the SSG predicted turbulence intensity at $X/H \geqslant 4$ are the reflections of the faster development of the shear layer and hence reduced level of turbulence generation, as is indicated earlier.

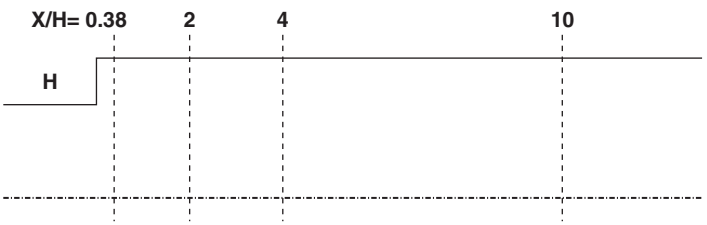

Figure 4. Geometry of sudden expanding pipe flow (H—step height).

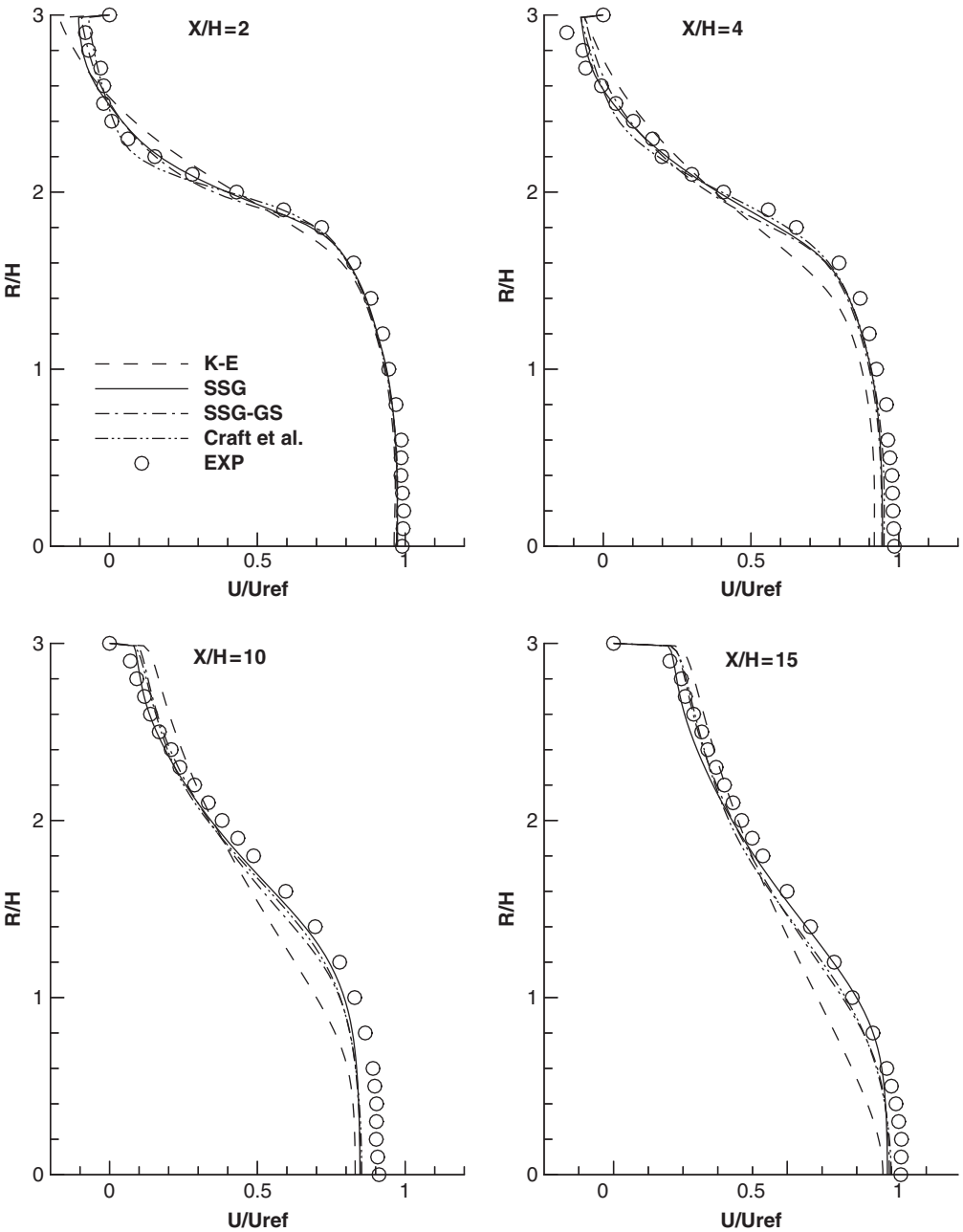

Figure 5. Axial velocity distributions of sudden expanding pipe flow.

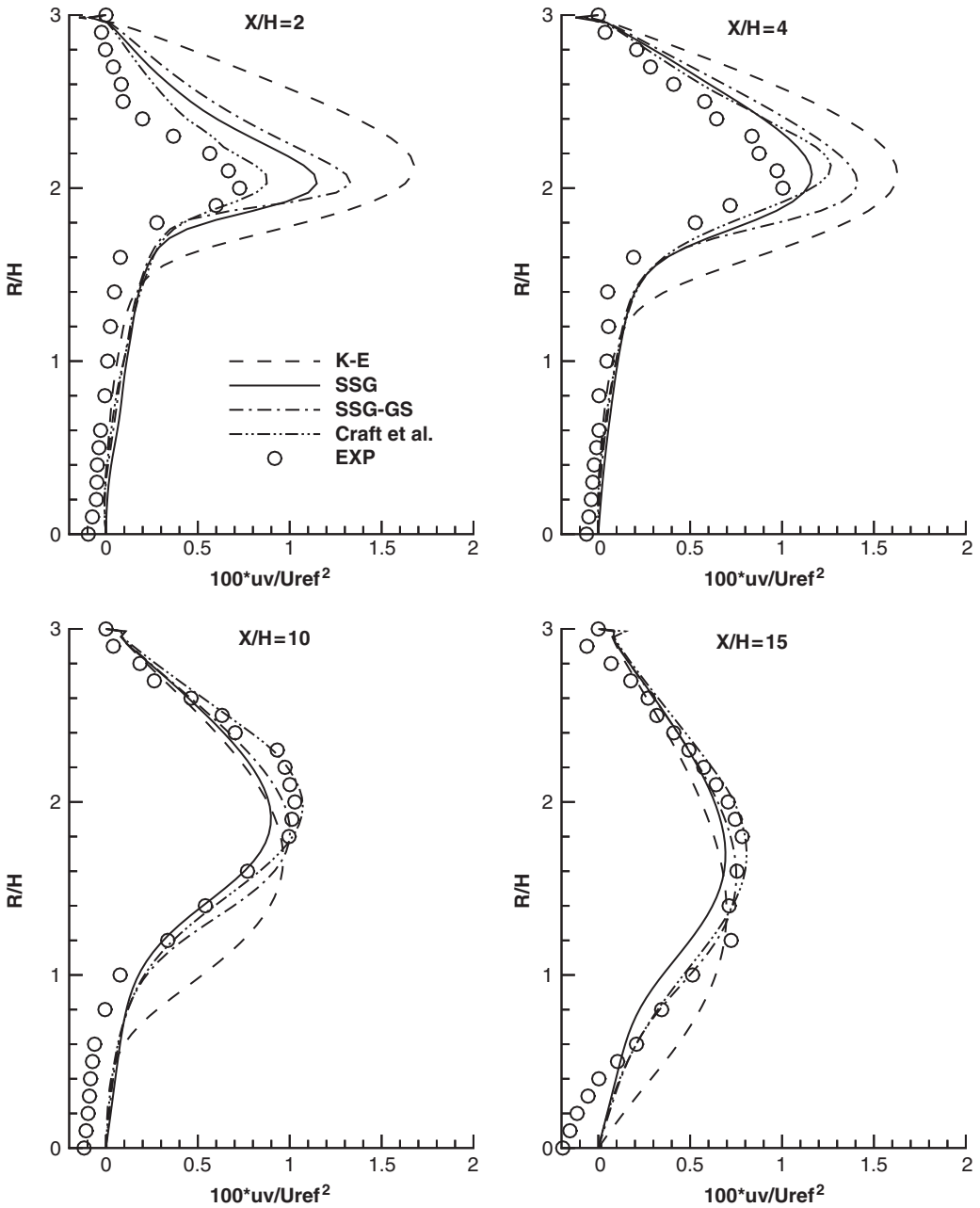

Figure 6. Shear stress.

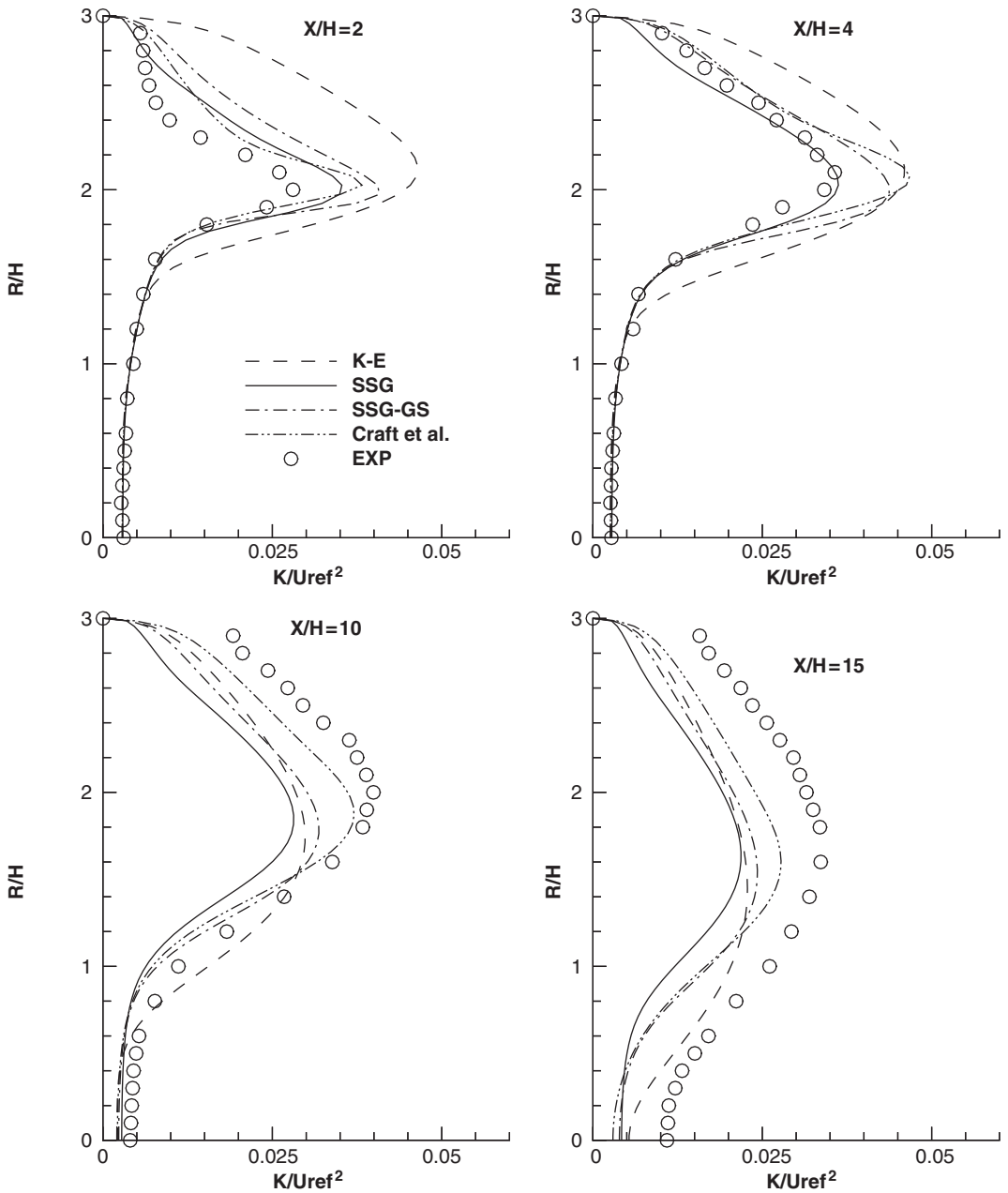

Figure 7. Turbulent kinetic energy distributions of sudden expanding pipe flow.

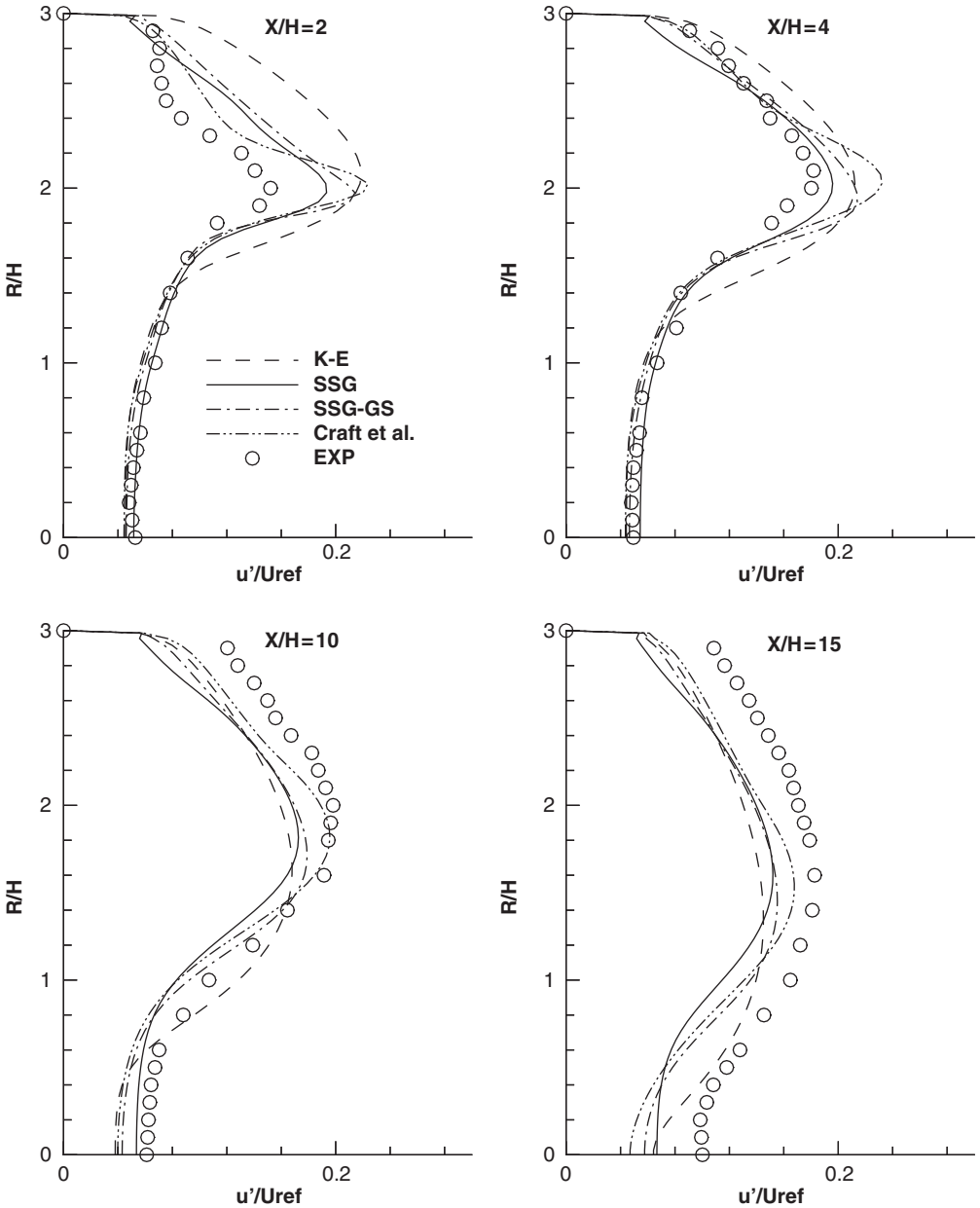

Figure 8. $\sqrt{\overline{u^2}}$ Distributions of sudden expanding pipe flow.

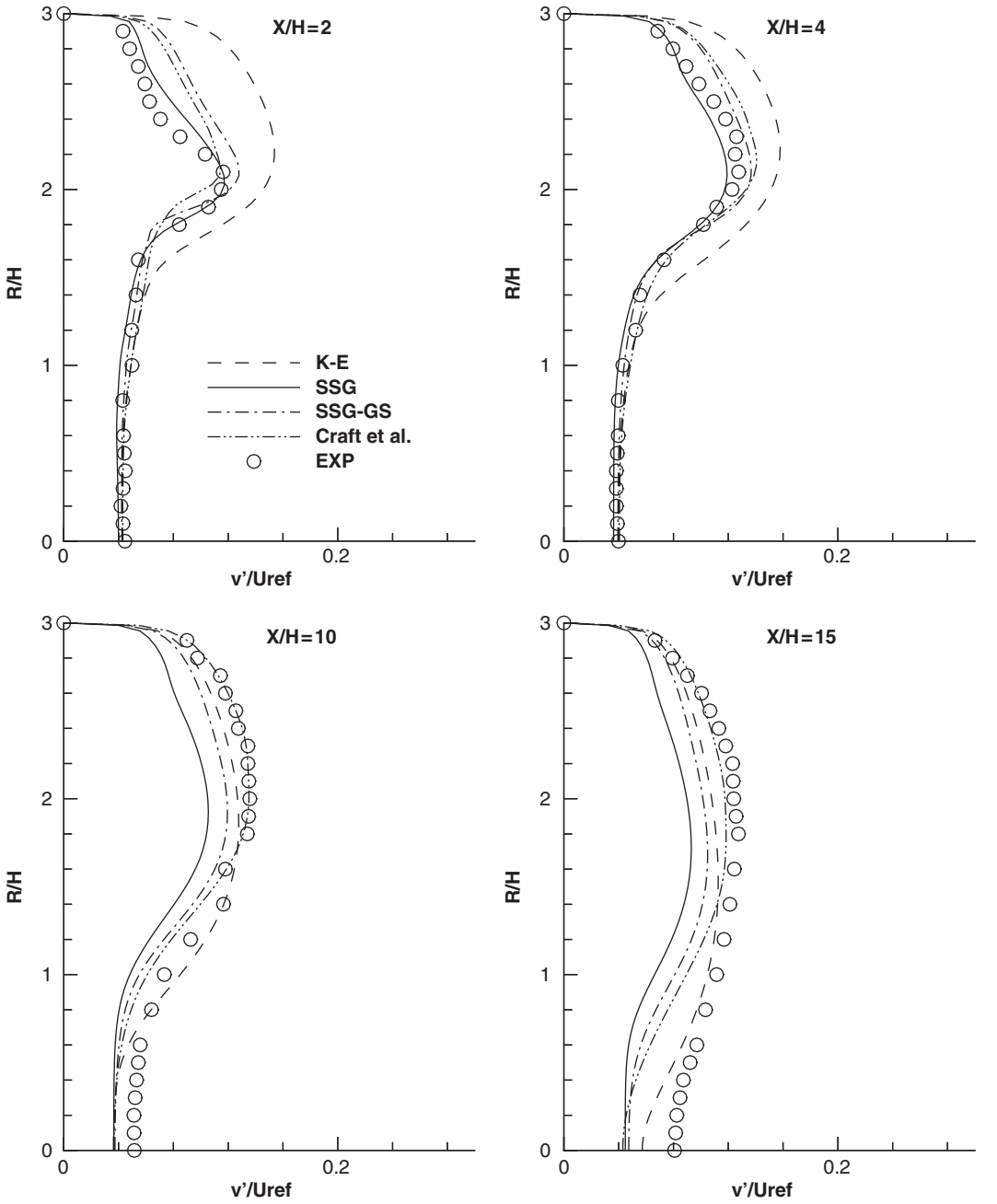

Figure 9. $\sqrt{\overline{v^2}}$ Distributions of sudden expanding pipe flow.

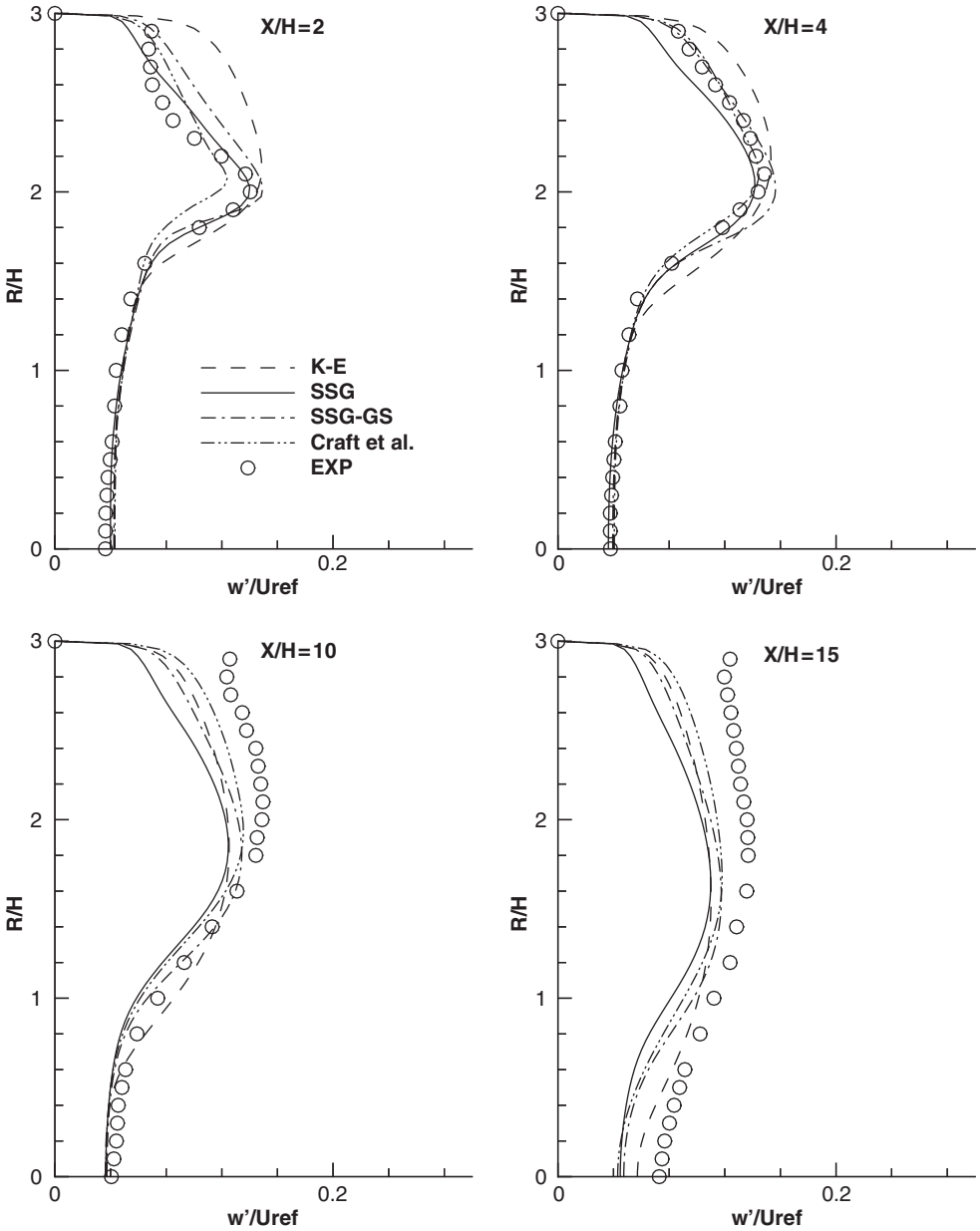

Figure 10. $\sqrt{\overline{w^2}}$ Distributions of sudden expanding pipe flow.

5. CONCLUSIONS

Capability of the explicit algebraic stress models to predict homogeneous and inhomogeneous shear flows are examined in the present study. For the homogeneous shear flow, all the models perform reasonably well, though at higher and lower strain rates the models behave differently. The importance of the explicit solution of the production to dissipation ratio is highlighted by examining the model performance at purely irrotational strain conditions. The regularized ASM (SSG–GS) was shown to produce unrealistic stress field under large irrotational strain, whereas the explicit ASM model (SSG) remains bounded. The stress field predicted by the anisotropic model though reasonable at lower irrotational strains, is not realistic at large strain rates and is also not bounded. Turbulent recirculating flows within sudden expanding pipes are further simulated with explicit algebraic stress model and anisotropic eddy viscosity model. Both models show a better stress–strain interaction, showing a reasonable shear layer development. The correct development of the shear layer is the reflection of the accurate shear stress level predicted. The anisotropic stress field are also accurately predicted by the models, though the Craft *et al.*'s model returns marginally better results.

ACKNOWLEDGEMENTS

This research work was supported by the National Science Council of Taiwan under grant NSC-89-2212-E-007-030 and the computational facilities were provided by the National Centre for High-Performance Computing of Taiwan which the authors gratefully acknowledge.

REFERENCES

1. Chen JC, Lin CA. Computations of strongly swirling flows with second-moment closure. *International Journal for Numerical Methods in Fluids* 1999; **30**:493–508.
2. Tsao JM, Lin CA. Reynolds stress modelling of jet and swirl interaction inside a gas turbine combustor. *International Journal for Numerical Methods in Fluids* 1999; **29**:451–464.
3. Shih TH, Zhu J, Lumely JL. A new Reynolds stress algebraic equation model. *Computer Methods in Applied Mechanics and Engineering* 1995; **125**:287–303.
4. Craft TJ, Launder BE, Suga K. Extending the applicability of eddy-viscosity models through the use of deformation invariants and non-linear elements. *5th International Symposium of Refined Flow Modelling and Turbulence Measurements*, Paris, 1993.
5. Shih TH, Zhu J, Liou WW, Chen KH, Liu NS, Lumely JL. Modeling of turbulent swirling flows. *11th Symposium of Turbulent Shear Flows*, Grenoble, 1997.
6. Gatski TB, Speziale CG. On explicit algebraic models for complex turbulent flows. *Journal of Fluid Mechanics* 1993; **254**:59–78.
7. Kuo NS, Lin YC, Lin CA. Computations of recirculating flows with non-linear eddy viscosity models. *3rd International Symposium on Turbulence, Heat and Mass Transfer*, Nagoya, Japan, 2000.
8. Rodi W. The prediction of free turbulent boundary layers by use of a two-equation model of turbulence. *Ph.D. Thesis*, University of London, 1972.
9. Pope SB. A more general effective-viscosity hypothesis. *Journal of Fluid Mechanics* 1975; **72**:331–340.
10. Girimaji SG. Fully explicit and self-consistent algebraic Reynolds stress model. *Theoretical and Computational Fluid Dynamics* 1996; **8**:387–402.
11. Speziale CG. Analytical methods for the development of Reynolds stress closures in turbulence. *Annular Review of Fluid Mechanics* 1991; **23**:107–157.
12. Speziale CG, Sarkar S, Gatski TB. Modeling the pressure-strain correlation of turbulence: an invariant dynamical system approach. *Journal of Fluid Mechanics* 1991; **227**:245–272.
13. Wallin S, Johansson AV. An explicit Reynolds stress model for incompressible and compressible turbulent flows. *Journal of Fluid Mechanics* 2000; **403**:89–132.
14. Patankar SV. *Numerical Heat Transfer and Fluid Flow*. Hemisphere Publishing Corporation: Washington, DC, 1980.

15. Leonard BP. A stable and accurate convective modelling procedure based on quadratic upstream interpolation. *Computer Methods in Applied Mechanics and Engineering* 1979; **19**:59–98.
16. Launder BE. Low-Reynolds-number turbulence near wall. *Report TFD/86/4*, Department of Mechanical Engineering, UMIST, U.K., 1986.
17. Rogers MM, Moin P. The structure of the vorticity filed in homogeneous turbulent flows. *Journal of Fluid Mechanics* 1987; **176**:33–66.
18. Champagne FH, Harris VG, Corrsin S. Experiments on nearly homogeneous shear flow. *Journal of Fluid Mechanics* 1970; **41**:81.
19. Harris VG, Graham AH, Corrsin S. Further experiments in nearly homogeneous turbulent shear flow. *Journal of Fluid Mechanics* 1977; **81**:657.
20. Tavoularis S, Corrsin S. Experiments in nearly homogeneous turbulent shear flow with a uniform mean temperature gradient. *Journal of Fluid Mechanics* 1981; **104**:311.
21. Chiu TH. Explicit algebraic stress modeling of homogeneous and inhomogeneous flows. *M.Sc. Thesis*, Department of Power Mechanical Engineering, National Tsing Hiua University, Hsinchu, Taiwan, 2001.
22. Craft TJ, Launder BE, Suga K. Prediction of turbulent transitional phenomena with a nonlinear eddy-viscosity model. *International Journal of Heat and Fluid Flow* 1997; **18**:15–28.
23. Ahmed SA, Nejad AS. Swirl effects on confined flows in axi-symmetric geometries. *Journal of Propulsion and Power* 1992; **8**:335–349.
24. Jones WP, Launder BE. The prediction of laminarisation with a two-equation model of turbulence. *International Journal of Heat and Mass Transfer* 1972; **15**:301–314.

